

## Effect of Electrode Type and Weld Current on Service Life of Resistance Spot Weld Electrode

Resul Önder Temiz<sup>1\*</sup> , Mert Onan<sup>1</sup> , E.Halit Çebi<sup>1</sup> , Salim Aslanlar<sup>2</sup> , and Şükrü Talaş<sup>3</sup> 

<sup>1</sup>Research and Development Centre, Yıldız Kalıp Company, İstanbul, 34555, Turkey

<sup>2</sup>Department of Metallurgical and Materials Engineering, Faculty of Technology, Sakarya University of Applied Sciences, Sakarya, Turkey

<sup>3</sup>Metallurgical and Materials Engineering, Faculty of Technology, Afyon Kocatepe University, Afyon, 03200, Turkey

### Abstract

HSLA steels are widely preferred in the automotive industry due to their advantages of high strength, lightening of vehicle weight and formability. The fact that a lot of welding processes are carried out during the creation of the vehicle body has made the welding operations of these steels an important topic. In this study, zinc coated HX340LAD+Z steel sheet material was welded by RSW in factory conditions using different electrode types. The welding operation was carried out with different current intensities and for 300 spot welds using three different electrodes with constant weld duration. After the welding trials, the shortening of the electrodes was examined and information about the electrode lifetime was obtained. The weld core diameter was measured on the sheet metal; micro-structure and microhardness investigations were also made in addition to the hardness of the weld nugget of dimensional stability. The splashing in the HX340LAD+Z material was investigated by SEM imaging and EDX studies. It was shown that F type Copper electrode was more efficient for RSW operation.

*Keywords:* HSLA steel; HX340LAD+Z; Resistance Spot Welding; Electrode life

### Research Article

#### History

Received 16.06.2023  
Revised 06.12.2023  
Accepted 31.12.2023

#### Contact

\* Corresponding author  
Resul Önder Temiz  
[resulondertemiz@gmail.com](mailto:resulondertemiz@gmail.com)  
Address: Research and Development Centre, Yıldız Kalıp Company, İstanbul, 34555, Turkey  
Tel:+902127711515

*To cite this paper:* Temiz R.Ö., Onan M., Çebi, E.H., Aslanlar, S., Talaş, Ş., Effect of Electrode Type and Weld Current on Service Life of Resistance Spot Weld Electrode. International Journal of Automotive Science and Technology. 2024; 8(1): 52-64. <https://doi.org/10.30939/ijastech..1315759>

### 1. Introduction

In the automotive industry, mild steels were predominantly used in vehicle production before the 1970s. Maximum formability and easy repairability of the chassis, which were design criteria for steels in 70s, were important factors in the selection of mild steels. The 1973 oil crisis experienced in the following period made reducing fuel consumption an important target. Reducing fuel consumption for automotive manufacturers has become possible because of the production of thinner and lighter parts and low weight vehicles. Vehicle production in this way has created a contradictory situation in terms of safety standards imposed on manufacturers [1]. Therefore, the demand for lighter and higher strength steels has increased in the automotive industry. High-strength steel (HSS) and advanced high-strength steel (AHSS) offer low cost, high strength, good formability, and outstanding crashworthiness compared to traditional steels [2]. The rapidly developing material technology of high-strength steels (HSS) over the time has also provided a significant competition against alternative materials (plastics, aluminum alloys, etc.) used for weight reduction in the automobile industry [3]. In the

study carried out within the scope of the Ultra-Light Steel Auto Body project (ULSAB) in 1994, 25% lightness, 14% cost saving and approximately 50% strength improvement advantages were achieved for 4-door sedan vehicles with the use of 90% HSS in the vehicle body [4]. In line with the benefits achieved through the utilization of HSS steels in vehicle body production and the emission reduction commitments outlined in the European Green Deal and the Paris Agreement in recent years, it is expected that the use of HSS in vehicle bodies will increase.

Another issue as important as the production of vehicle body elements as desired is the assembly of the body by combining pre-produced vehicle parts. The most preferred steel joining method in the automotive industry is resistance spot welding (RSW). The crash resistance of the vehicle is highly dependent on the accuracy and mechanical performance of the resistance spot welds [5]. Resistance spot welding (RSW) is based on joining sheet metals between two electrodes by applying high current and force. In the meantime, due to the resistance of the material against the current, overheating occurs and a weld pool is formed. With the formation of the weld pool, the current is cut off and pressure is applied to the partially molten area with the

electrode pressure force. When the weld pool of the materials cools and solidifies, the joining process is completed [6]. The size of the weld nugget diameter depends on the weld force, weld time, material being spot welded and the thickness of sheet material. While increasing the welding current, a successful welding can be achieved with a reduced time, but high current can cause spatters during the welding operation. The success of the weld diameter obtained after spot welding affects the weld quality and electrode life. Softening of electrode, electrode diameter expansion, cavitation on the electrode surface and recrystallisation that occur in the electrode bulk and its effect on its service life are among the main problems [7]. Besides as the number of welds increases, the contact resistance between the electrode and workpiece at high temperature increases the risk of chemical contamination and pitting on the surface of electrode due to repeated loading and releasing routine. This situation accelerates with further operations and results in an asymmetrical contact surface and increased contact resistance in general. Therefore, the current density is affected and the probability of undesired arcing increases. A consequence of this is the poor welding quality [8, 9]. Therefore, the quality, cost and welding time of resistance spot welding is an important issue in the automotive industry in many respects. The realization of the welding process at the desired quality and speed in mass production is directly related to the life of the electrode. Decreased electrode lifetime and their performance may result in production and vehicle safety risks such as poor welding quality, loss of time, maintenance and replacement costs.

In this study, zinc coated HX340 LAD+Z HSLA steel sheet was joined by spot welding process using three different current levels and three different electrode types at service conditions. Optical and SEM imaging were used to define the characteristics of spot welds.

## 2. Material and Method

The HX340 LAD+Z coded HSLA (High Strength Low Alloy) hot dip galvanized micro alloyed steel sheets were provided from ERDEMİR Inc. Co. in rolls, with the dimensions of 1500 x 640 x 6 mm. The rolls are sliced into desired sizes at Yıldız Kalıp Company. The chemical composition of the steel is given in Table 1 by weight percentage. The effect of zinc coating present on the steel sheet on spot weld was also investigated. Sample cutting was carried out by a laser cutting device to prepare the sample cutting and spot welding from the sheet material of 1500 x 900 x 1.5 mm size. The areas of the spot welding on the plates were divided 50 x 50 mm sections thus the plates made ready for the welding process. In Figure 1, the image of the sample divided into sections is presented. Spot welding was carried out by using three types of electrodes with different tip forms with a fixed inner diameter of 16 mm, which are the most widely used in the automotive industry. The images of 3 different types of electrodes used in this study are presented in Figure 2.

Table 1. Material HX340LAD+Z (HSLA) Chemical composition (wt. %) and mechanical properties of the material

| Chemical Composition |       |       |                        |       |       |              |       |
|----------------------|-------|-------|------------------------|-------|-------|--------------|-------|
| %C                   | %Mn   | %P    | %S                     | %Si   | %Al   | %V           | %Nb   |
| 0.074                | 0.623 | 0.018 | 0.006                  | 0.010 | 0.043 | 0.035        | 0.040 |
| Yield Strength (MPa) |       |       | Tensile Strength (Mpa) |       |       | Elongation % |       |
| 396.2                |       |       | 471.7                  |       |       | 27.0         |       |

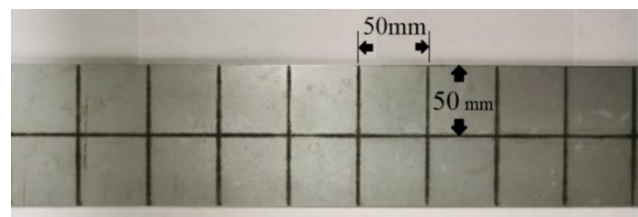


Fig. 1. Volume HX340 LAD+Z sample divided into sections.

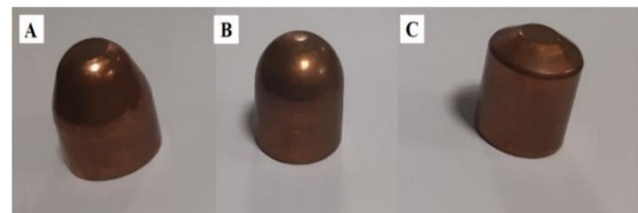


Fig. 2. Different types of electrodes selected for the study; a) G, b) F and c) B

The parameters used during spot welding of HX340 LAD+Z sheet samples are; current (A), welding current time (ms) and electrode type. In practice, the welding current time is kept constant as 300 ms and therefore experiments were carried out for each electrode type with variable current levels. Before proceeding to the experiments, resistance spot welding for all electrode types was tested on the sheet material and the parameters where spatter did not occur were determined for better performance hence the interaction regarding the parameters are restricted. Experimental parameters were grouped and the joining was carried out using Mactera brand 120 kV RSW machine at predetermined current values for each of the electrode types. In this study, three different geometrical types of electrodes with Cu-CrZr chemical composition were used, e.g. G, B and F as in Fig.2. Selected parameters for the spot welding are given in Table 2.

Table 2. Selected electrode types and spot-welding parameters.

| Electrode Type | Specimen Code | Duration (ms) | Current (kA) |
|----------------|---------------|---------------|--------------|
| G              | G65           | 300           | 6,5          |
|                | G70           |               | 7,0          |
|                | G75           |               | 7,5          |
| B              | B72           | 300           | 7,2          |
|                | B77           |               | 7,7          |
|                | B82           |               | 8,2          |
| F              | F60           | 300           | 6,0          |
|                | F65           |               | 6,5          |
|                | F70           |               | 7,0          |

Electrode tips that performed 300 spot welding processes and sheet metal samples containing the 300th spot weld were prepared for microstructural examination. The spot-welded area was sliced in half with an abrasive cut-off disc, mounted in Bakelite and polished. For the polishing process, 220G sandpaper was initially used and the surfaces were sanded up to 1200G and then brought to a mirror shine by using 1 µm Alumina powder. After polishing, the surface was etched with 1% Nital to reveal the microstructure. Optical images were obtained from the spot weld sections using an Olympus optical microscope, electron microstructure imaging was performed using SEM-LEO 1430 VP electron microscope device, and then elemental analysis with the RÖNTEC QX2 EDX device attached to the SEM device.

After imaging and elemental analysis, microhardness measurement was carried out using the SHIMADZU HMV-2 device with a 50 g load for the duration of 10 s. Microhardness measurement was made on three different locations and the evaluation of overall hardness was made over the average value. With the dimensional measurements on the spot weld, sheet metal and the electrode tip were obtained for further analysis. Dimensional measurement of spot weld is presented in Figure 3.

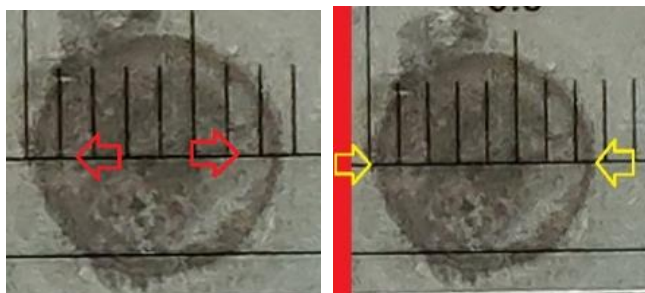


Fig. 3. Weld outer diameter including HAZ (left) and weld core center diameter (right).

### 3. Results and Discussion

This section contains the results and discussion of resistance spot welding performance of HX340 LAD+Z steel sheet and electrodes. Welding current was selected as the resistance spot welding parameter, and its range was determined according to the spatter-free welding performance prior to this study. Dimensional measurements and microscopic imaging were performed under the same conditions for all samples. Dimensional measurement results are presented in Tables 3 and 4.

Table 3. Dimensional measurement (mm) results of spot welds and electrodes according to the electrode type, A) the outer diameter of the weld core formed on the sheet plate (including HAZ) and the outermost diameter measurement results of the electrode used in welding, B) the core diameter of the weld core formed on the sheet metal and the effective electrode weld surface diameter measurement results.

| Electrode Type     | Weld  |        |         | Electrode |        |         |       |
|--------------------|-------|--------|---------|-----------|--------|---------|-------|
|                    | Width | Length | Average | Width     | Length | Average |       |
| A (Outer Diameter) |       |        |         |           |        |         |       |
| G                  | G65   | 9,00   | 9,00    | 9,00      | 10,30  | 11,20   | 10,75 |
|                    | G70   | 9,40   | 9,10    | 9,25      | 11,00  | 11,10   | 11,00 |
|                    | G75   | 9,10   | 9,20    | 9,15      | 10,20  | 10,30   | 10,25 |
| B (Core Diameter)  |       |        |         |           |        |         |       |
| G                  | G65   | 6,80   | 7,20    | 7,00      | 8,10   | 8,20    | 8,15  |
|                    | G70   | 6,70   | 7,10    | 6,90      | 9,00   | 8,20    | 8,60  |
|                    | G75   | 7,00   | 7,10    | 7,05      | 10,20  | 8,20    | 8,15  |
| A (Outer Diameter) |       |        |         |           |        |         |       |
| B                  | B72   | 9,00   | 7,30    | 8,15      | 9,10   | 9,10    | 9,10  |
|                    | B77   | 8,70   | 8,20    | 8,45      | 10,90  | 10,90   | 10,90 |
|                    | B82   | 8,10   | 9,00    | 8,55      | 9,70   | 9,30    | 9,50  |
| B (Core Diameter)  |       |        |         |           |        |         |       |
| B                  | B72   | 7,10   | 5,60    | 6,35      | 8,00   | 8,00    | 8,00  |
|                    | B77   | 6,80   | 5,80    | 6,30      | 7,80   | 7,30    | 7,55  |
|                    | B82   | 5,90   | 6,90    | 6,40      | 7,90   | 6,40    | 7,15  |
| A (Outer Diameter) |       |        |         |           |        |         |       |
| F                  | F60   | 6,70   | 7,10    | 6,90      | 8,20   | 7,30    | 7,75  |
|                    | F65   | 7,00   | 7,00    | 7,00      | 9,10   | 7,80    | 8,45  |
|                    | F70   | 7,20   | 7,00    | 7,10      | 7,90   | 8,20    | 8,05  |
| B (Core Diameter)  |       |        |         |           |        |         |       |
| F                  | F60   | 5,50   | 5,50    | 5,50      | 6,10   | 6,00    | 6,05  |
|                    | F65   | 6,00   | 5,80    | 5,90      | 6,90   | 5,70    | 6,30  |
|                    | F70   | 5,40   | 5,10    | 5,25      | 5,90   | 6,10    | 6,00  |

The G-type electrode tip is designed to create a uniform pressure and allows homogeneous distribution of the compression force. With the increasing current intensity at the tip, the heat input also increases, and it is seen in Table 3 that the increase in the heat input partially raises the weld core diameter. With increasing current, the weld core depth and the outer diameter of the resistance spot weld core also increased. While the difference between average outer diameter and the average weld core diameter in the highest heat input and the lowest heat inputs in type G and B electrodes was 2.15 and 2.20 mm, respectively, in series of F type electrode, the nugget size difference in samples with the average highest and the average lowest heat input was 2.40 mm. As is known, the heat input causes a decrease in the modulus of elasticity and yield point in metallic materials and increases its plasticity at temperatures above 600 °C giving a peak at 730 °C [10, 11]. Therefore, with increasing current, an increase in core depth and an increase in the outer diameter of the RSW core were observed. When the results

were compared with the literature, the highest current value of 7.6 kA for H34LOAD+Z were observed for successful welding and similar values for all types of electrodes were attempted in our experiments [12]. It was determined that there was no significant change in the electrode contact surface dimensions. In RSWs, the wear in any part of the components are primarily affected by the temperature due to the resistance between the electrode and sheets and hence the oxidation is the result of this high temperature. The second effect is the deformation of sheets that usually occurs due to the repeated applied force in the weld zone during the RSW operation. The deformation acts in many ways such that it accelerates oxidation as the surface area is increased due to thinning of sheets and the surface oxide layer is deformed and broken open for fresh reaction with air. The wear mechanism occurring on the electrode is the mixture of high temperature oxidation, the deformation and also the formation of CuZn intermetallics. Cyclic fatigue is generated during the spot-welding operation resulting in a pitting and subsequent material loss, which ends with large cavity [13]. The compression force with the assistance of heat will eventually deform the electrode tip and change its shape in long run. In Table 3, it is evident that the width-to-width ratio values in B-type electrode tip forms are very close to 1 and show a homogeneous deformation and wear. It is clearly seen that F-type electrode tip tests give better results compared to the G-type electrode tips which also produce good results. The HAZ area of the welds made with electrode type F is narrower, which is an advantage when the weld strength is considered as it applies more force per unit area, assuring a very

close contact between the sheets of metals at high temperatures. With increasing heat input, this difference has widened more.

Table 4. Measuring the variations in electrode heights (mm)

| Electrode Type | UBE | UTE   | BEAW  | TEAW  | DCBE  | DCTE |       |
|----------------|-----|-------|-------|-------|-------|------|-------|
| G              | G65 | 21,86 | 22,02 | 21,71 | 22,03 | 0,15 | -0,01 |
|                | G70 | 21,96 | 22,08 | 21,88 | 22,09 | 0,08 | -0,01 |
|                | G75 | 21,88 | 22,86 | 21,77 | 21,85 | 0,11 | 0,01  |
| B              | B72 | 22,02 | 21,95 | 21,96 | 21,93 | 0,06 | 0,02  |
|                | B77 | 21,92 | 21,95 | 21,88 | 21,95 | 0,04 | 0,00  |
|                | B82 | 21,95 | 21,92 | 21,94 | 21,96 | 0,01 | -0,04 |
| F              | F60 | 22,32 | 22,20 | 22,13 | 22,16 | 0,19 | 0,04  |
|                | F65 | 22,29 | 22,26 | 21,96 | 22,12 | 0,33 | 0,14  |
|                | F70 | 22,96 | 22,19 | 22,22 | 22,12 | 0,04 | 0,07  |

The parameters in Table 4 are respectively; electrode type, unused bottom electrode (UBE), unused top electrode (UTE), bottom electrode after welds (BEAW), top electrode after welds (TEAW), dimensional change in bottom electrode (DCBE) and dimensional changes in top electrode (DCTE). Table 4 shows the height of the electrodes before and after RSW welding operations. Although there are no substantial changes in the welding electrode dimensions before and after welding (Table 4), the F-type electrode produced the most shape changes according to Table 4 when the changes in dimensions are concerned. Due to the shape of the G-type electrode, it can play an important role in the deformation since it has more flat projection surface and narrower area which facilitates deformation and reduces the core thickness, instead of forming a more stable contact surface as in the B-type electrode. An increased wear of the lower electrodes or reduced electrode length is believed to be associated with increased heat input. Figure 4 shows the spot welds made by G, B and F type of electrodes, respectively. Figure 4a and c, i.e. G and F type of electrodes, are believed to be less affected by the pressure from the electrode however showed the most deformed weld core, however, the weld core made by B type electrode produced flat surface with a sharp change in contrast along the edge to the right.

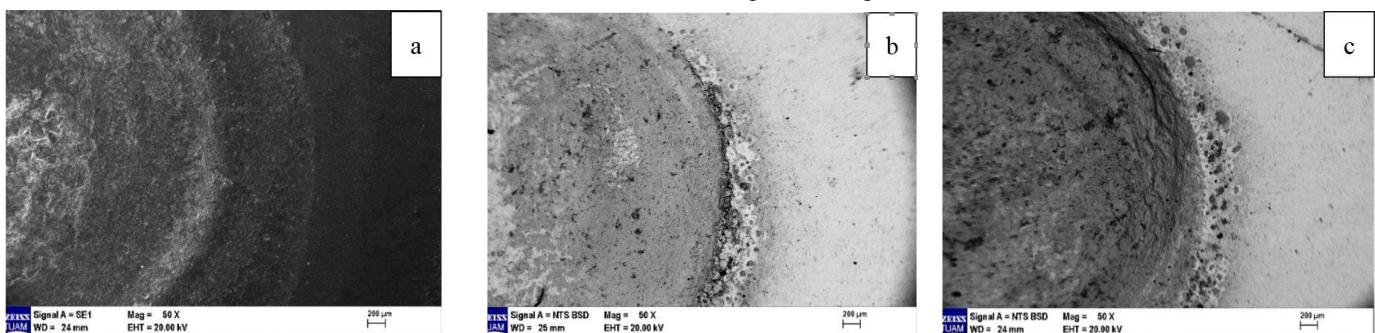


Fig. 4. SEM images of the welds made with the three forms of electrode tip; a) G65, b) B77 and c) F65.

Contrary to the F and G type electrodes, the high amount of wear may be due to the fact that the electrode is completely Zinc coated, allowing the formation of CuZn compound on the electrode surface and being more easily exposed to mass wear. Although no investigation has been made on this subject, the absence of Copper on the B-type electrode surfaces and the fact that only Zinc is seen in very high amounts points in this direction. For the G Type electrode, it is concluded that there is no significant copper transfer from the electrode surface to the steel sheet because Copper is encountered on the surface, but this amount is very small. Considering the other two electrode profiles, low copper transfer in this electrode type is a very important factor in reducing electrode wear. Although the elemental distribution is generally homogeneous, it is gathered that a condensation and accumulation of Zinc vapor on the surface of Cu electrode occurs as a result cooling of electrode and [14] and its being trapped in the pores on the surface by evaporation.

Microhardness measurements taken from the weld section of sheet materials are given in Table 5. The effect of the F-type electrode on the microhardness is quite evident. Hardness values increase on average. The main parameter of the systematically increasing microhardness values is the variable grain size, and the intragranular morphology that emerges with the latter. In addition, it was determined that the result of microhardness measurements was very low due to the softening of the spot resistance welding electrodes.

Table 5. Average Microhardness (HV<sub>0.05</sub>) results of resistance spot welded samples.

| Electrode type | Specimen code | Standard deviation | Average hardness (HV <sub>0.05</sub> ) |
|----------------|---------------|--------------------|----------------------------------------|
| G              | G65           | 31,47              | 258,71                                 |
|                | G70           | 3,63               | 245,70                                 |
|                | G75           | 8,14               | 261,14                                 |
| B              | B72           | 45,16              | 311,07                                 |
|                | B77           | 23,04              | 321,34                                 |
|                | B82           | 9,49               | 299,77                                 |
| F              | F60           | 5,88               | 360,03                                 |
|                | F65           | 29,35              | 378,39                                 |
|                | F70           | 21,64              | 376,76                                 |

### 3.1. Electron microscope analyzes of electrode and weld surface

SEM images of the weld core and electrode of the F60, F65 and F70 specimens, as well as the EDX results taken from the surface are given in Figure 5- Figure 7 a-d in which the resistance spot weld core depth can be easily seen together with elemental mapping. The HAZ region, on the other hand, is approximately 1.2 mm out of the core edge. According to the elemental change observed on the spot weld cores, it is seen that Zinc and Copper transfer takes place. Particularly at high temperatures, the mass transfer takes place mainly by evaporation (applies to Zinc) and adhesively

deposited to the surface. Wear on the electrode surfaces, which occurs due to mass transfer by adhesion to the surface, can be seen in Figure 5.

In this study, between Figure 5 and 7, there is Zinc accumulation on all surfaces, and there is little or no mass transfer of Copper. It is thought that this transfer, adhesion to very hot surfaces with cyclic weld process, occurs via insulated Copper fragments. Copper is an element that is difficult to heat because of its high heat capacity and high coefficient of thermal conduction; due to this feature, when used as an electrode, it is cooled very easily, but, it allows deformation even under low forces since it is very soft metal. Since they do not show a well-defined fatigue limit, rupture becomes easier and regions that show local deformation in each thermal cycle break with high current density and thermal density. These two transfer differences appear as an effective mechanism in this electrode type and other types of electrodes.

As a result of the examination of the EDX analysis values given in Figures 5 and 6, it is seen that Zinc and Copper are randomly distributed and Aluminum is also present. In some coatings, Aluminum can be found together with Zinc. Aluminum is possibly transferred from the coating on steel surface and evaporated together with the Zinc and accumulated to the surface of the weld zone.

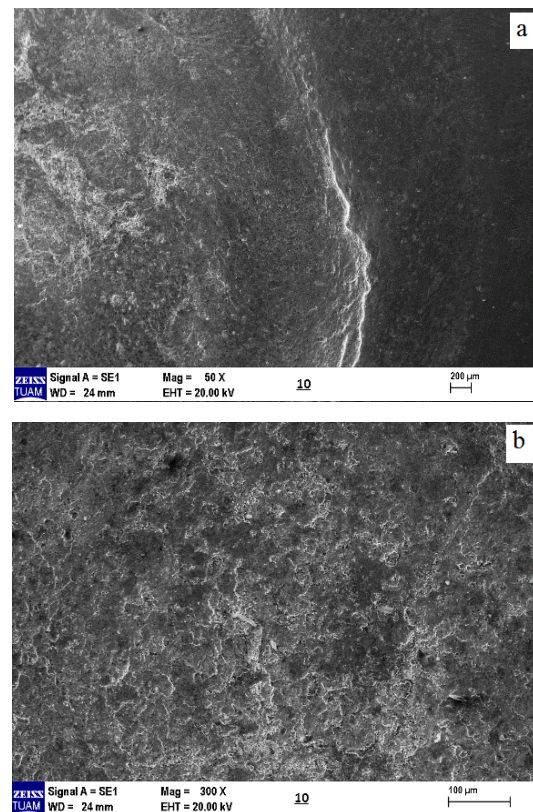


Fig. 5. SEM macro (a) and micro (b and c) images and (d) elemental mapping images of the weld core of sample G65.

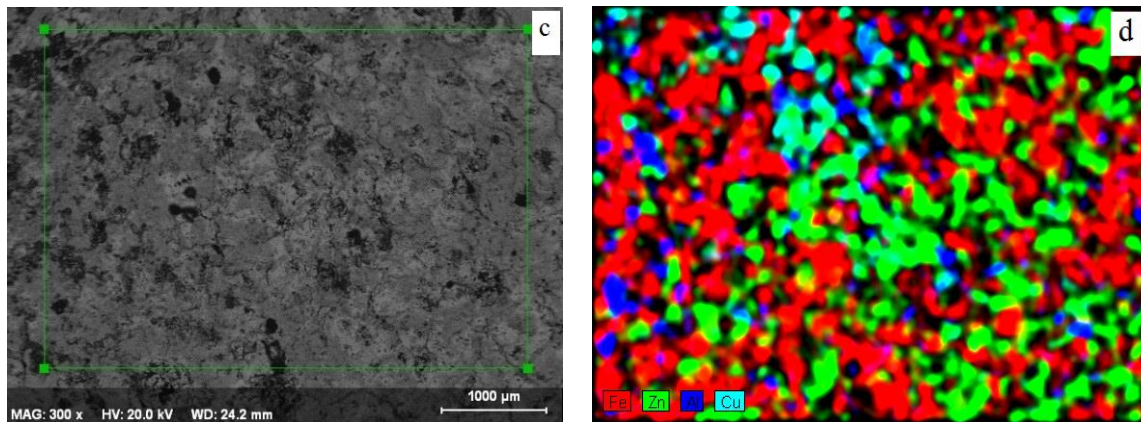


Fig. 5. SEM macro (a) and micro (b and c) images and (d) elemental mapping images of the weld core and (c) electrode of sample G65.

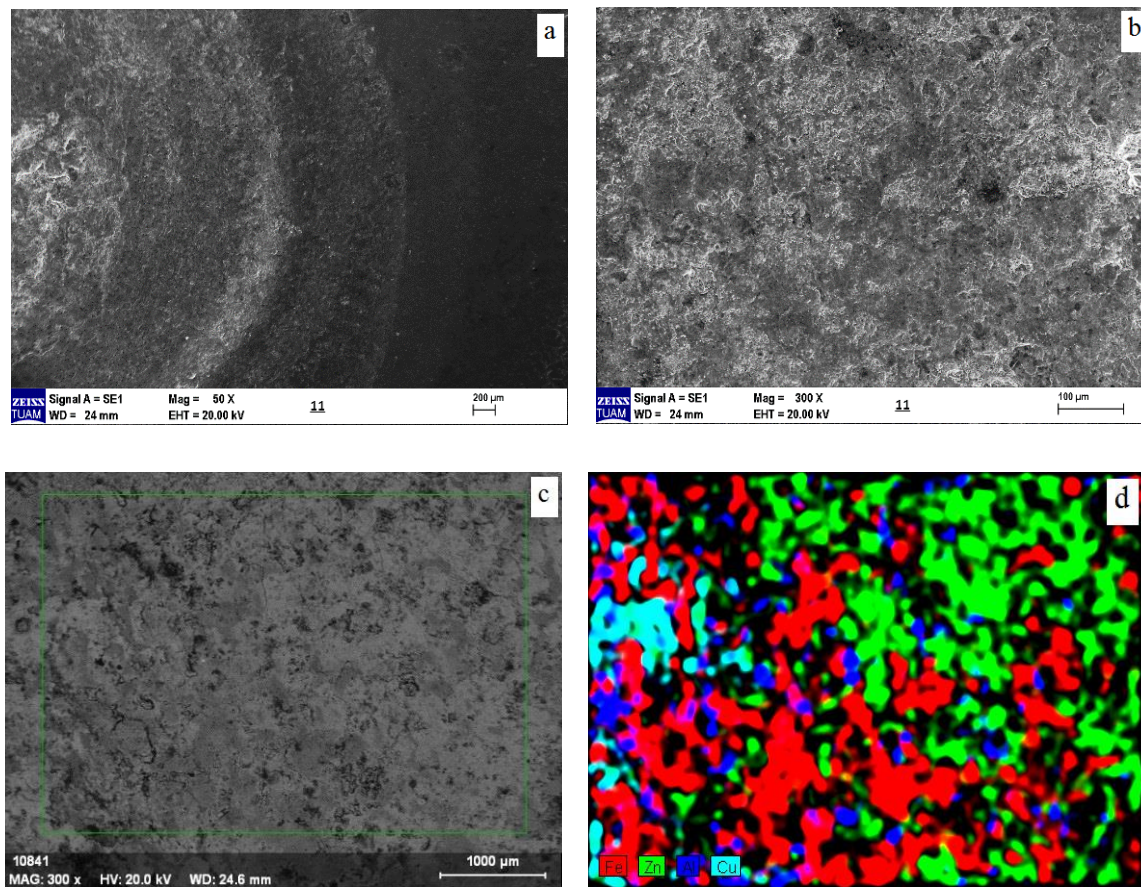


Fig. 6. SEM macro (a) and micro (b and c) images and (d) elemental mapping images of the weld core and (c) electrode of sample G70.

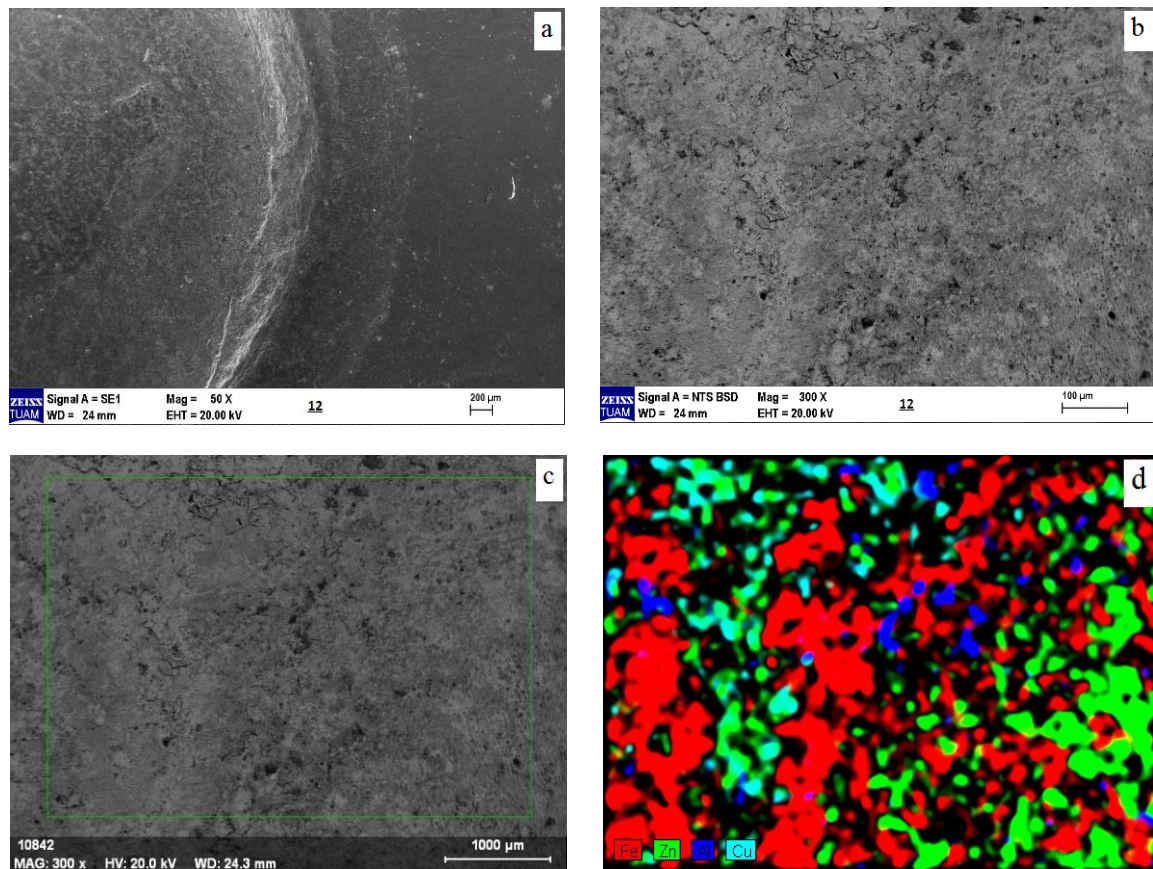


Fig. 7. SEM macro (a) and micro (b and c) images and (d) elemental mapping images of the weld core and (c) electrode of sample G75.

In order to support the above-mentioned Copper transfer, it is given in Figure 8 d that the Copper ratio is transferred at a higher rate with the increasing current. Since the Oxygen elemental spots are in low amounts and corresponding approximately 14–25 % of total composition, it is readily assumed that oxides of Zinc and Aluminum are more likely to form in place of Copper, according to Ellingham diagram of oxide [15]. When the reaction atmosphere contains oxygen during welding exposure at room temperature, ZnO starts to form first then  $\text{Cu}_2\text{O}$  is transformed into CuO directly [16]. The decomposition of CuO, which has two decomposition temperatures e.g. 982 °C for  $\text{Cu}_2\text{O}$  and 1070 °C for  $\text{Cu} + \frac{1}{2}\text{O}_2$ , is thermodynamically unstable with increasing temperature, pure Copper is obtained when 1070 °C is reached and facilitates the adhesion to the hot steel surface [17]. It is likely that the transfer of Copper to the weld surface is through oxide path and decomposition of oxides of Copper is less likely to occur since there is a repeated heating on the surface. The detection of Copper may also be due to the presence of oxides of Copper as it is not distinguished by the detector but rather together with oxygen peaks.

Spot weld zone images and EDX elemental mapping analyzes

made with B type electrodes are given in Figure 8-10 a-d. The analyses indicate that a very serious accumulation of Zinc on the surface of electrode or its transfer via a contact on the surfaces occurred. The absence of Copper transfer is probably related to the thickness of the oxide layer formed on the electrode surface or the difficulty in creating a clean surface. As a result of the evaporation of the Zinc element, more Zinc can adhere to the Copper surface and can be beneficial in forming a barrier against the spot weld core and preventing the transfer of Copper to the weld surface. Therefore, in this series, copper transfer did not occur at significant level and the amount of Zinc was observed at very high levels. The problem with this series is that both the weld core and the electrode surfaces are subjected to more wear due possibly to high temperature deformation process. As it can be seen in Figure 10, unlike the F and G type electrodes, the high amount of wear may be due to the fact that the electrode is completely coated with Zinc, allowing the formation of CuZn compound and is more easily exposed to mass wear; the absence of Copper presence on the surfaces and Zinc is in very high amounts points in this direction.

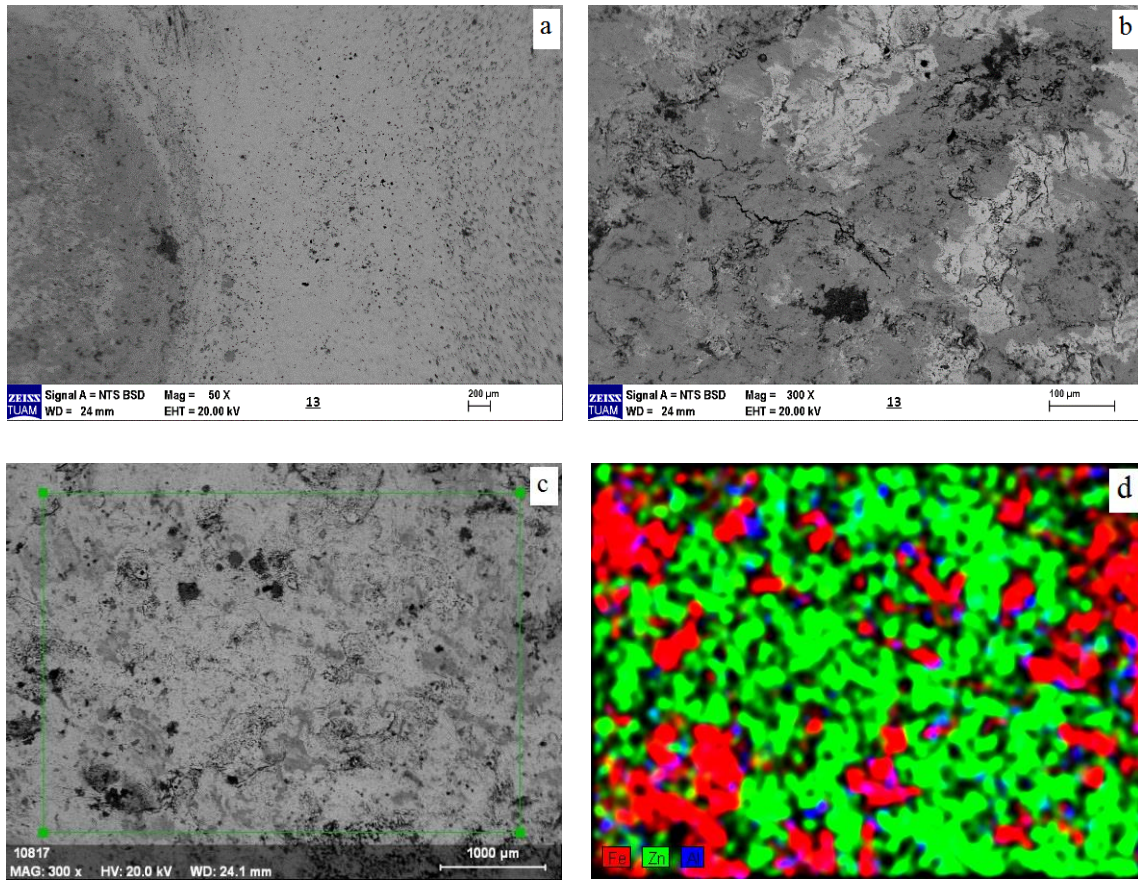


Fig. 8. SEM macro (a) and micro (b and c) images and (d) elemental mapping images of the weld core and (c) electrode of sample B72.

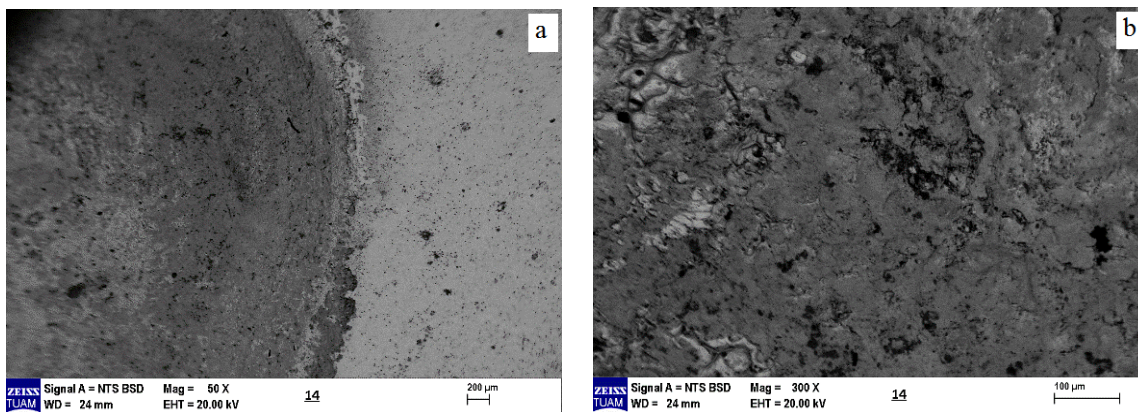


Fig. 9. SEM macro (a) and micro (b and c) images and (d) elemental mapping images of the weld core and (c) electrode of sample B77.



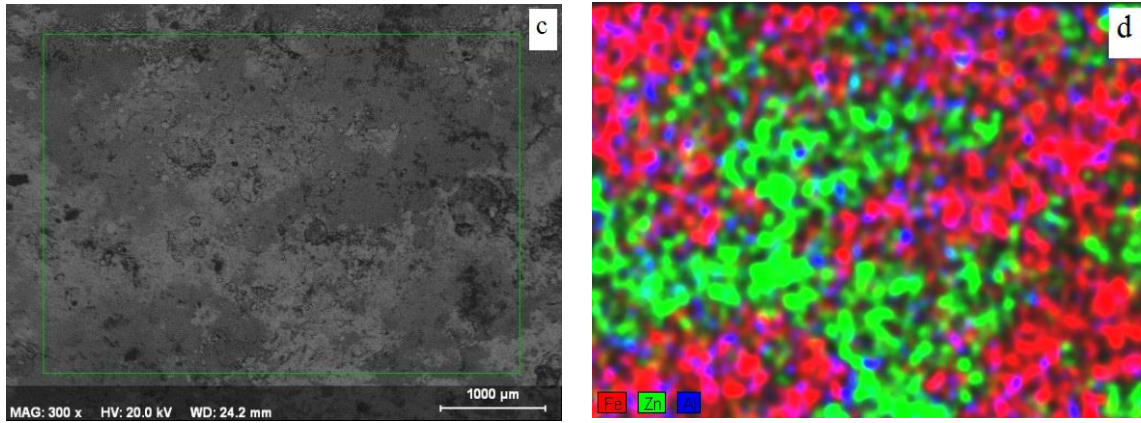


Fig. 9. SEM macro (a) and micro (b and c) images and (d) elemental mapping images of the weld core and (c) electrode of sample B77.

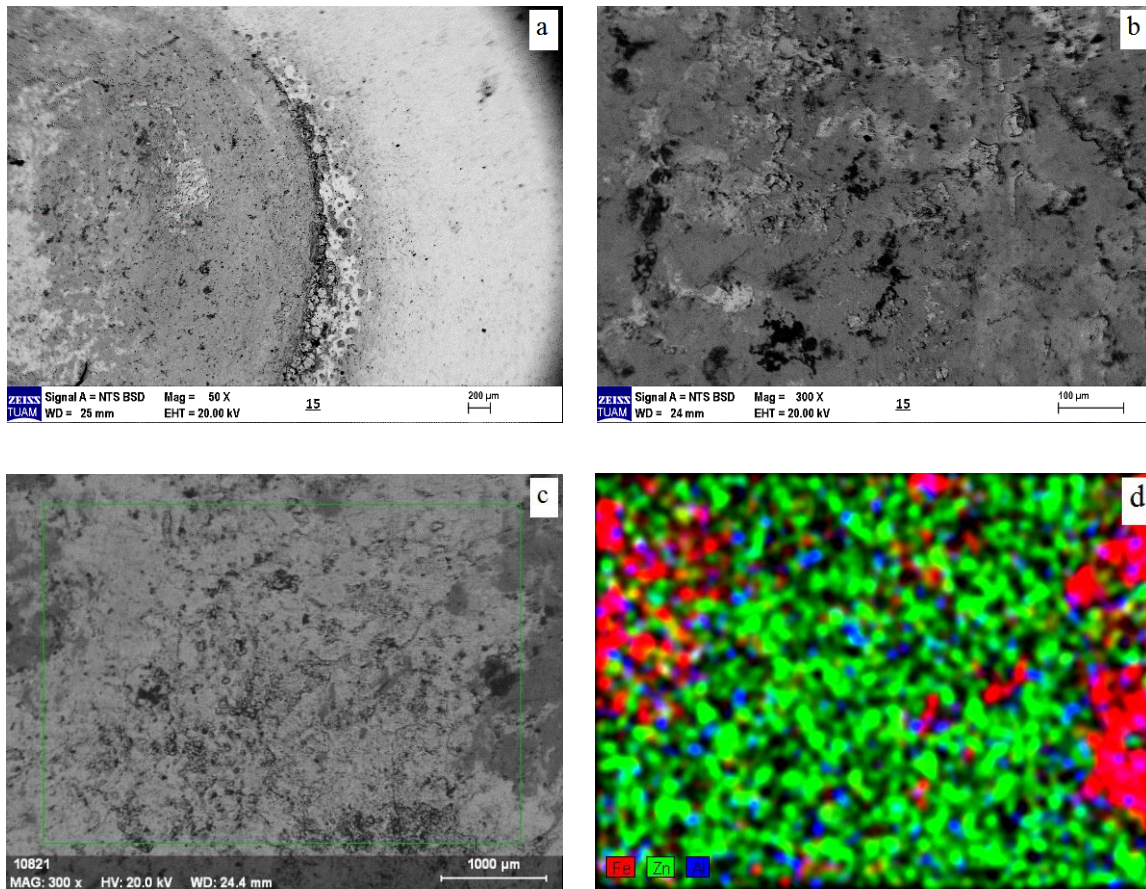


Fig. 10. SEM macro (a) and micro (b and c) images and (d) elemental mapping images of the weld core and (c) electrode of sample B82.

Electron microscope images and EDX analysis of the test samples made with G type electrodes are given in Figures 11 – 13 a-d. In EDX analysis, it is observed that the amount of Copper and Zinc elements decrease on the surface. Although the elemental distribution is generally homogeneous, it is thought that it condenses and accumulates as a result of the presence of Zinc in the wear pores on the surface, the formation of Zinc vapor on the surface and its trapping in the pores by evaporation. It is possible that the reason for the less wear on the surface of this electrode type is that the electrode composition or shape leads to less exposure to damage by fatigue and oxidation, or that these pores are covered with more Zinc compounds or oxides and prevent copper transfer. Another important mechanism is the co-existence of Copper and Zinc on the electrode surface, which appeared in the last specimen (Figure 11 and elemental mapping image in Figure 13 d), which can be presented as evidence for the formation of CuZn compound. As the weld current increases the amount of Zinc and Aluminium spots appear to have increased due to high volatilization of respective elements and concentrated near and in the voids on the surface.

As seen in Figure 13 d, Copper was also detected, however, there was no high amount of copper transfer to the weld surface. Considering the other two electrode profiles, low copper transfer in this type of electrode e.g. F type, is a very important property in reducing electrode wear but it is more associated with the amount of low evaporation of Zinc which leads to a reduced formation of Zinc rich layer on electrode surface that may eventually cause micro fatigue ruptures on the surface due to repeated compression force along with high temperature.

It may be also due to the shape of the electrode, too, which allows the vapor of Zinc escape from the surface of the electrode, leaving less amount of Zinc accumulating on the surface. As it can be seen in the images given in Figures 6, 7 and 8, the F type electrode is considered to be a more feasible electrode because it gives a clean surface appearance with less Copper transfer. It is a preferred feature that the shape of the electrode reduces the contact with the evaporating Zinc and reduces its transfer to the RSW surface and the electrode surface. The surface of electrode would eventually lead to the formation of brittle phases and cause the electrode crack before its typical service life.

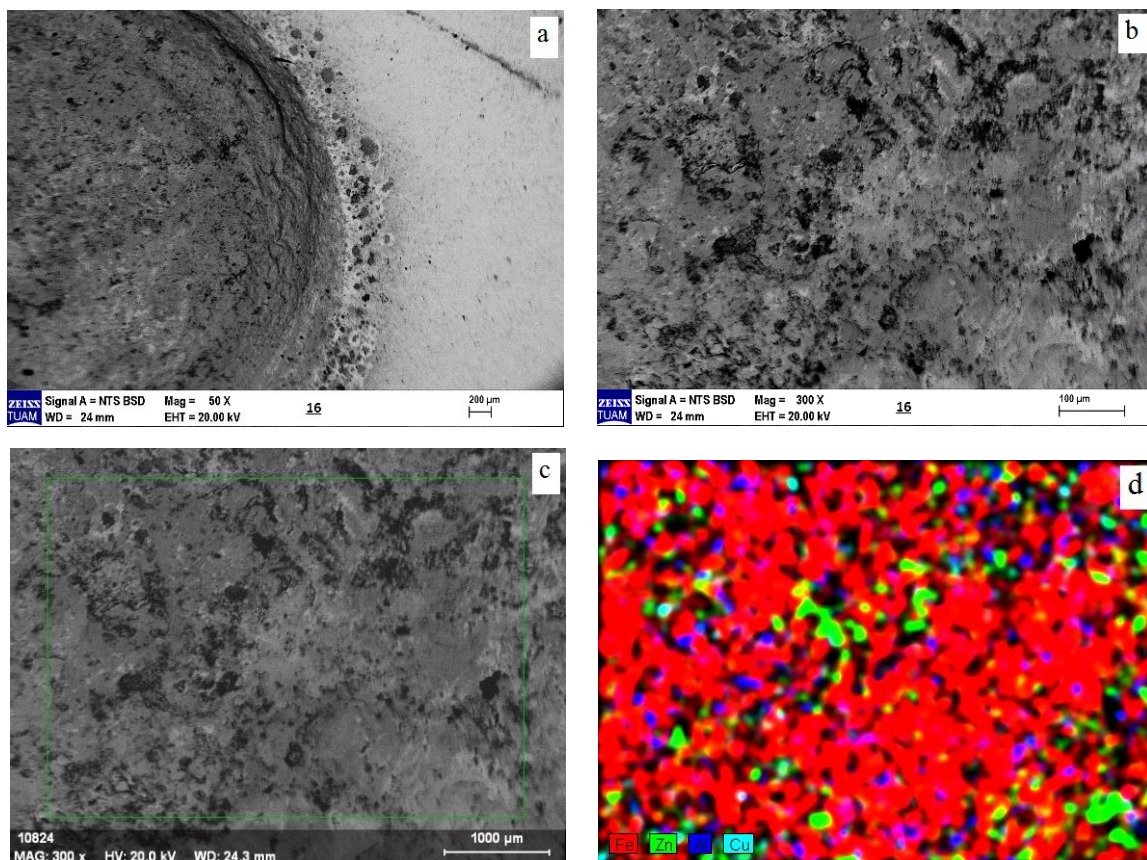


Fig. 11. SEM macro (a) and micro (b and c) images and (d) elemental mapping images of the weld core and (c) electrode of sample F60.

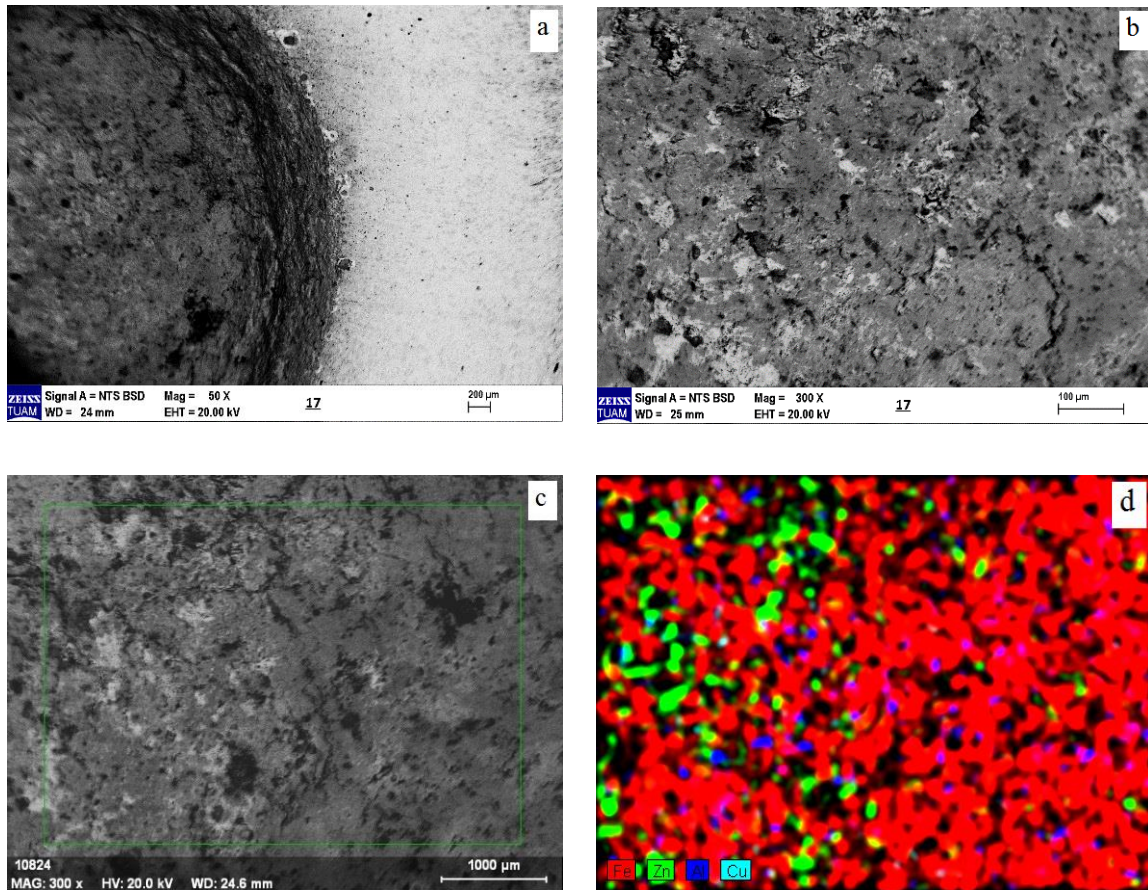


Fig. 12. SEM macro (a) and micro (b and c) images and (d) elemental mapping images of the weld core and (c) electrode of sample F65.

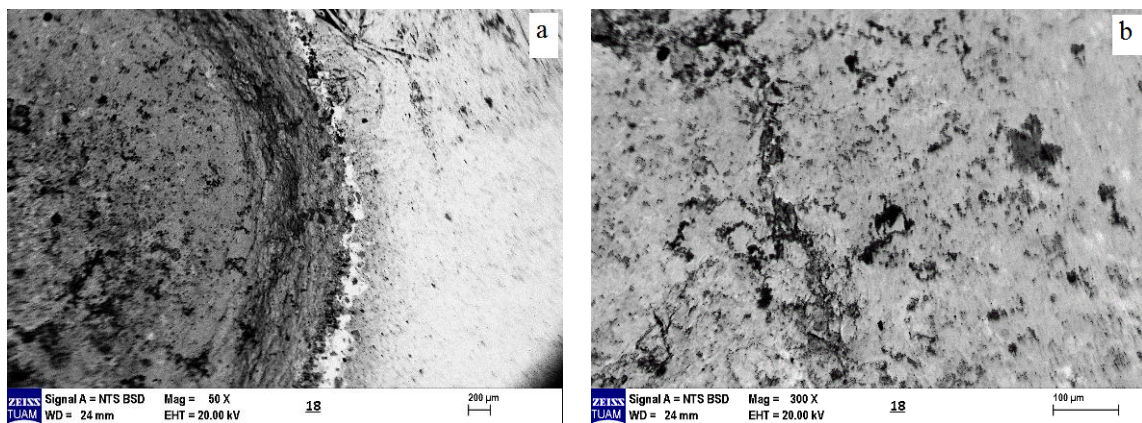


Fig. 13. SEM macro (a) and micro (b and c) images and (d) elemental mapping images of the weld core and (c) electrode of sample F70.

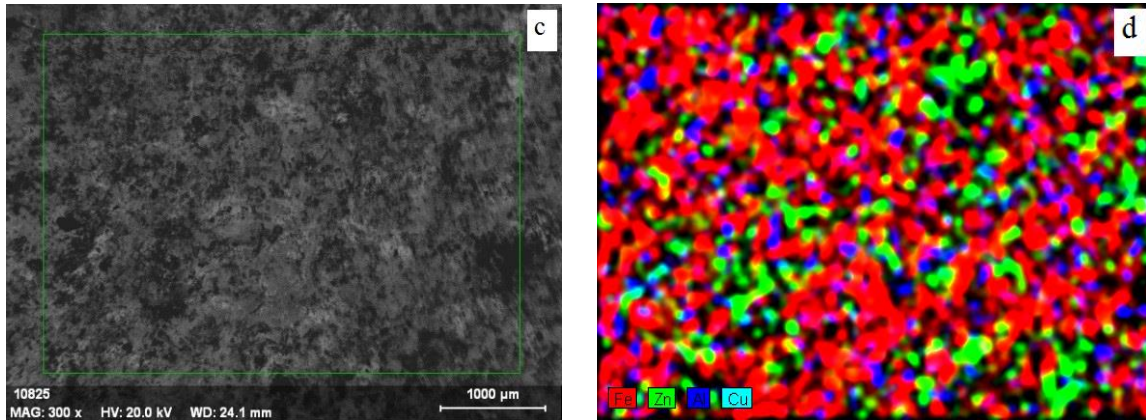


Fig. 13. SEM macro (a) and micro (b and c) images and (d) elemental mapping images of the weld core and (c) electrode of sample F70.

#### 4. Conclusions

In this study, HX340LAD+Z material with high mechanical properties was successfully welded by RSW techniques. As a result of the physical and microstructural examinations of the weld area and the electrode surface, the following conclusions were reached:

- In the experiments with the electrode tips, better results were obtained from the G-type electrode, which was found to have a good performance in terms of least amount of Zinc accumulation on the surface of electrode.
- Resistance spot welding electrodes are resistant to high temperature applications and show deformation over the time depending on the pressure created during welding and the frequency of welding.
- Weight loss can be observed in the electrode material as a result of alloying with Zinc, which helps the formation of Zinc rich compound which breaks away under the compression force.
- G-type electrode has a significant effect on micro hardness and the hardness value increases on average with the order of G, B and F, respectively.

#### Acknowledgment

This study was supported by Yıldız Kalıp Company. Therefore, we would like to thank Yıldız Kalıp Company and its employees.

#### Nomenclature

|      |                                             |
|------|---------------------------------------------|
| BEAW | : Bottom electrode after welds (mm)         |
| EDX  | : Energy Dispersive X-Ray analysis          |
| DCTE | : Dimensional changes in top electrode (mm) |
| HSLA | : High strength low alloy steel             |
| HSS  | : High-strength steels                      |
| SEM  | : Scanning electron microscope              |
| TEAW | : Top electrode after welds (mm)            |
| UBE  | : Unused bottom electrode (mm)              |
| UTE  | : Unused top electrode (mm)                 |

#### Conflict of Interest Statement

The authors declare that there is no conflict of interest in the study.

#### CRediT Author Statement

**Resul Önder Temiz:** Supervision, Conceptualization, Drafting the article, Formal analysis,  
**Mert Onan:** Conceptualization, Drafting the article, Data curation, Formal analysis,  
**E.Halit Çebi:** Data curation, Formal analysis,  
**Salim Aslanlar:** Intellectual content, Formal analysis, Data curation,  
**Şükrü Talaş:** Conceptualization, Data curation, Validation, Intellectual content

#### References

- [1] Lesch C, Kwiaton N, Klose FB. Advanced high strength steels (ahss) for automotive applications – tailored properties by smart microstructural adjustments. *Steel Research International*. 2017;88(10):1700210. <https://doi.org/10.1002/srin.201700210>
- [2] Kuziak R, Waengler RK&S. Advanced high strength steels for automotive industry. *Archives Of Civil And Mechanical Engineering*. 2008;8:103-117. [https://doi.org/10.1016/S1644-9665\(12\)60197-6](https://doi.org/10.1016/S1644-9665(12)60197-6)
- [3] Beardmore P. The potential for high strength steels in the u.s. automotive industry. *Materials & Design*. 1981;2(5):250-259. [https://doi.org/10.1016/0261-3069\(81\)90068-6](https://doi.org/10.1016/0261-3069(81)90068-6)
- [4] Galán J, Samek L, Verleysen P, Verbeken K, Houbaert Y. Advanced high strength steels for automotive industry. *Revista De Metalurgia*. 2012;48(2):118-131. <https://doi.org/10.3989/revmetalm.1158>
- [5] Pouranvari M, Ranjbarnoodeh E. Failure mode of hsla/dqsk dissimilar steel resistance spot welds. *Ironmaking & Steelmaking*. 2013;40(4):276-281. <https://doi.org/10.1179/1743281212Y.0000000044>
- [6] Raut M, Achwal V. Optimization of spot welding process parameters for maximum tensile strength. *International Journal Of Mechanical Engineering And Robotics Research*. 2014;3(4):506-517. <https://doi.org/10.18178/ijmerr>
- [7] Pouranvari M, Asgari HR, Mosavizadch SM, Marashi PH, Goodarzi M. Effect of weld nugget size on overload failure mode of resistance spot welds. *Science and Technology of Welding and Joining*. 2013;12(3):217-225. <https://doi.org/10.1179/174329307X164409>
- [8] Wei P, Wu T, Chen L. Joint quality affected by electrode contact condition during resistance spot welding. *Ieee Transactions On*

- Components, Packaging And Manufacturing Technology. 2013; 3(12):2164 - 2173. <https://doi.org/10.1109/TCPMT.2013.2284497>
- [9] Xing B, Yan S, Zhou H, Chen H, Qin QH. Qualitative and quantitative analysis of misaligned electrode degradation when welding galvanized steel. The International Journal of Advanced Manufacturing Technology. 2018;97:629-640. <https://doi.org/10.1007/s00170-018-1958-1>
- [10] Gulyaev AP, Sarmanova LM. High-temperature plasticity of carbon steels. Metal Science And Heat Treatment. 1972;14:329-332. <https://doi.org/10.1007/BF00657023>
- [11] Rezaeian A, Keshavarz M, EH. Mechanical properties of steel welds at elevated temperatures. Journal of Constructional Steel Research. 2020;167:105853. <https://doi.org/10.1016/j.jcsr.2019.105853>
- [12] Viňáš J, Kaščák L, Greš M. Optimization of resistance spot welding parameters for microalloyed steel sheets. Open Engineering. 2016;6(1):504-510. <https://doi.org/10.1515/eng-2016-0069>
- [13] Vural M, Akkuş A, Eryürek B. Effect of welding nugget diameter on the fatigue strength of the resistance spot welded joints of different steel sheets. Journal of Materials Processing Technology. 2006;176(1-3):127-132. <https://doi.org/10.1016/j.jmatprotec.2006.02.026>
- [14] Arghavani M, Movahedi M, Kokabi A. Role of zinc layer in resistance spot welding of aluminium to steel. Materials & Design. 2016;102:106-104. <https://doi.org/10.1016/j.matdes.2016.04.033>
- [15] Buschow K.H.J. Encyclopedia of materials. Science and technology. Elsevier; 2001
- [16] Huh, D. Electrode Life and Weldability Improvement in Resistance Spot Welding of DP600 [Master's thesis]. University of Waterloo; 2017.
- [17] Yi F, Delisio JB, Nguyen N, Zachariah MR, Lavan DA. High heating rate decomposition dynamics of copper oxide by nanocalorimetry-coupled time-of-flight mass spectrometry. Chemical Physics Letters. 2017;689:26-29. <https://doi.org/10.1016/j.cplett.2017.09.066>